

Bleomycin-induced modulations of PARP 1 activity, NAD⁺ and PARG content in rat lung nuclei

I. G. Artsruni, A. L. Asatryan, K. S. Matinyan

Yerevan State University, Yerevan, Armenia

Article info

Received 04.01.2024

Received in revised form
05.02.2024

Accepted 07.02.2024

Yerevan State University,
Yerevan, 0025, Armenia.
Tel: +3-746-071-05-24.
E-mail:
anush.asatryan@ysu.am

Artsruni, I. G., Asatryan, A. L., & Matinyan, K. S. (2024). Bleomycin-induced modulations of PARP 1 activity, NAD⁺ and PARG content in rat lung nuclei. *Regulatory Mechanisms in Biosystems*, 15(1), 102–106. doi:10.15421/022415

Bleomycin-induced lung pathology in rodents is a well recognized animal model widely used for evaluation of new therapeutic approaches in treatment of lung inflammation and fibrotic diseases. It is documented that poly(ADP-ribose)polymerase 1 activity has a significant role in development of inflammatory processes in the heart, liver and brain. Herein, we used biochemical and immunochemical methods for estimation of poly(ADP-ribose)polymerase 1 (PARP 1) activity, NAD⁺ and poly(ADP-ribose)glycohydrolase (PARG) protein content in rat lung nuclei during the inflammatory phase in a bleomycin-induced one-hit rat model. To evaluate the influence of bleomycin – induced alterations in DNA structure on regulation of poly(ADP-ribose)polymerase 1 activation pathways, we isolated DNA from nuclei of lung tissues in the phase of acute lung inflammation induced by bleomycin, and DNA melting profiles were investigated. In the present study we investigated whether naturally occurring water-soluble polyphenol tannic acid with widely accepted anti-fibrotic and anti-inflammatory effects can influence poly(ADP-ribose)polymerase 1 activity, NAD⁺ and poly(ADP-ribose)glycohydrolase protein content in nuclear fraction isolated from rat lung tissues in a bleomycin-induced acute lung injury model. It was demonstrated that NAD⁺ level and poly(ADP-ribose)glycohydrolase protein content decreased in rat lung nuclei during the inflammatory phase in the bleomycin-induced acute lung injury model. Treatment of rats with tannic acid enhanced the effects displayed by bleomycin in lung nuclei, thus indicating synergistic interaction with the drug in the field covering PARP 1 activity, poly(ADP-ribose)glycohydrolase (PARG) protein and NAD⁺ content in lung nuclei. We observed PARP 1 inhibition in nuclei of lung tissue during the inflammatory phase in the bleomycin-induced acute lung injury rat model, which could be coupled with the drop of NAD⁺ level in nuclei. In the present study we highlighted that bleomycin (BLM) can induce DNA destabilization in lung nuclei. It was proposed that bleomycin-induced modulations in DNA structure could hamper PARP 1 binding with DNA and down-regulate the enzyme activating pathway in lung nuclei. The role of poly(ADP-ribose)glycohydrolase depletion in lung nuclei and sequential accumulation of poly(ADP-ribose)polymers in lung cells, which triggers their destruction and tissues damage, was proposed. It is suggested that in the light of synergistic interaction between bleomycin and tannic acid (TA) the anti-inflammatory role of tannic acid should be repurposed.

Keywords: single challenge bleomycin rat model; poly(ADP-ribose) polymer metabolism; tannic acid; DNA melting profiles; activity regulation pathways.

Introduction

PARP 1 is a chromatin-associated multifunctional enzyme involved in a broad spectrum of structural and functional activities responsible for genomic integrity, DNA repair, transcriptional activity, cell survival and death (Gupte et al., 2017). The enzyme is an abundant nuclear protein with complex modular structure. PARP 1 catalyzes NAD⁺ hydrolysis to nicotinic amide and ADP-ribose moieties with sequential transfer of ADP-ribose units to serine, tyrosine and glutamic acid residues localized to the auto-ribosylation domain of the enzyme molecule (auto-polyADP-riboseylation) and to acceptor proteins in the vicinity of PARP 1 (trans-polyADP-riboseylation). Poly(ADP-ribose)polymers (PARp) are formed by sequential addition to the first protein-bound unit of other ADP-ribose moieties via 2'OH of the ribose residue. The linear stretches of PARp usually branch every 20–50 ADP-ribose units. Branching occurs at the 2'' OH of the ribose moieties. High negative charge of PARp strands affect protein structure and functions (Demény & Virag, 2021). Activity of PARP 1 dramatically increased when it binds to DNA free ends via ZI and ZII Zn-fingers, localized to specific DNA-binding domain of the enzyme molecule (D'Amours et al., 1999). The most intriguing feature of PARP 1 is its ability to undergo auto-poly(ADP-riboseylation) (auto-PARylation) within the auto-modification domain. Introduction of negatively charged PAR

chains into the auto-PARylation domain of the enzyme results in destabilization of the molecular microenvironment and weakens PARP 1 affinity for DNA. In the DNA damage repair process, short-term binding of PARP 1 to DNA free ends occurs and PARP 1 activation attracts repair proteins which initiate DNA repair pathway to a specific point, where PARP 1 molecule turned to a mechanical obstacle for repair machinery. Heavily auto-PARylated PARP 1 molecules dissociate from DNA-binding sites (Muthurajan et al., 2014), thus enabling repair proteins to localize in the site of DNA damage and complete damage repair (Hopkins et al., 2019). When the loosened state of chromatin is required for the free access to DNA in relatively prolonged processes (e.g. transcription, DNA replication), accumulation of highly polyADP-ribosylated chromatin-associated proteins is needed (Tulin et al., 2003). This is achieved due to PARP 1 binding to specific non-B DNA structures (e.g. distortions in the DNA helical backbone, unpaired regions of double-strand DNA, cruciform and hairpins). Interactions of PARP 1 with non-B DNA structures lead to sequential catalytic activation of auto-PARylation and trans-PARylation of chromatin associated proteins even in the absence of DNA free ends (Lonskaya et al., 2005; Edwards et al., 2021). Chromatin loosening is maintained by continuous PARP 1 activation via interaction of C-terminal domain of the enzyme with histone H4 (Thomas et al., 2019). It has been proposed that different functions of PARP 1 are coordinated by

interactions between different domains of the enzyme molecule and their targets (Langelier et al., 2018). Once bound to DNA in the presence of an inhibitor, PARP 1 remains bound (it is “trapped”) onto chromatin, hindering many chromatin-associated functions. In the case of DNA lesions PARP 1 trapping accelerates replication fork collapse and progression of double-strand breaks (Pommier et al., 2016). Dynamic association and dissociation of PARP 1 chromatin play a crucial role in regulation of many chromatin-associated functions and PARP 1 trapping has a detrimental effect on vital functions in cells.

Cancer cells are prone to proliferation and often bear defective DNA damage repair systems. In this context, inhibition of PARP 1 enzymatic activity came into focus as a promising strategy in chemotherapy of cancer patients treated with DNA damaging agents (alkylating agents, UV- and X-ray treatment). At present, four PARP 1 inhibitors (PARPis) olaparib, talazoparib, niraparib and rucaparib are approved for clinical use and they are exploited as single agent therapy or in combination chemotherapeutic regimen in treatment of cancer patients. The clinical impact of PARP 1 inhibitors is not limited to cancer therapy but also reaches pathologies that are characterized by inflammation (Berger et al., 2017). It was reported that the level of protein PARylation increased in lung tissues of BLM challenged mice and preclinical data revealed therapeutic benefits of PARP 1 inhibition in multiple models of acute lung injury (Lucarini et al., 2017; Pazzaglia & Pioli, 2020; Szabo et al., 2020). However, the extent of protein PARylation in cells depends on dynamic balance between cellular PARPs and the enzymes responsible for PAR degradation i.e. poly(ADP-ribose)glycohydrolase (PARG) and ADP ribosyl hydrolase 3 (Harrison et al., 2020). Thus, it should be taken into account that the level of protein PARylation is determined by complex interplay of functionally linked enzymes responsible for PAR synthesis and degradation i.e. PARP 1 and PARG. Coming from this, we were interested in examining whether BLM could directly affect PARP 1 activity, PARG protein and NAD⁺ content in nuclear fraction of BLM-challenged rat lung tissues. It is well documented that BLM causes DNA single- and double-strand breaks which cease replication and transcription. In addition, BLM can bind to DNA by intercalation of its bithiazole unit between DNA bases within the DNA minor groove (Murray et al., 2018). Considering the role of DNA in PARP 1 activating mechanisms we were interested in examining whether BLM can induce structural changes in nuclear DNA isolated from lung tissues.

Naturally occurring water-soluble polyphenol tannic acid (TA), which has been exploited for centuries as an anti-inflammatory agent, attenuates fibrotic alterations in the liver (Chu et al., 2016; Reed et al., 2019). In the present study we investigate whether anti-fibrotic and anti-inflammatory effects of TA could be associated with its effects on PARP1 activity, PARG and NAD⁺ content in lung tissues of rat in the inflammatory phase of BLM-induced acute lung injury.

Materials and methods

Animals and treatments. Wistar albino male rats (6 weeks old) weighing 100–120 g were used throughout the experiments. The animals were obtained from stock of the animal house of YSU Biology Faculty, fed with standard diet and water ad libitum, and housed in plastic cages at 20 °C with a 12-hr light/dark cycle. The animals were cared for and used according to the Guide for the care and use of laboratory animals (Guide for the care and use of laboratory animals, 8th edition. Washington (DC), National academies press (US), 2011). The experimental protocols were designed in compliance with the National Centre of Bioethics (Armenia) and the European Community regulations on animal experimentation for scientific purposes (D.M. 116192; O.J. of E.C. L358/1 12/18/1986). The experiments were approved by the local Animal Ethics Committee (Yerevan State University).

The animals were standardized by weight and divided randomly into three different groups of 12 animals each. The first group was treated with intra-peritoneal injection 200 µL of saline and was referred to as the control group. To induce acute lung inflammation, the second group of rats was injected with BLM (Med chem express, USA, lot: hy-17565/cs-3071, 2023). 2 U/kg of BLM diluted in 200 µL of saline was delivered by single intra-peritoneal injection. The third group rats were injected with

TA (Sigma Aldrich, # 1401-55-4, USA, 2023) (10 mg/kg in 200 µL of saline) 24 hours after BLM administration and daily during the next seven days. Delivery of TA was interrupted on day 8 after BLM challenge and the experiments proceeded for a further seven days (up to day 15 after BLM injection).

Nuclei isolation from lung tissues. The rats were killed after anesthesia with ethyl ether and their lungs were harvested immediately postmortem. For isolation of the nuclei lungs were minced on ice and homogenized in 0.25 M sucrose buffered with 20 mM Tris containing 15 mM NaCl, 60 mM KCl, 0.15 mM spermine and 0.5 mM spermidine. Nuclei were isolated according to Hewish and Burgoyne (Hewish & Burgoyne, 1973). Purified lung nuclei were suspended in isolation media and normalized to 1 mg DNA/mL content. In *in vitro* experimental settings biochemical measurements were conducted after incubation of the lung tissues' nuclei of the control group animals for 2 hours in media, where 10 µM BLM or TA was added when necessary.

Estimation of intra-nuclear NAD⁺ content. Nuclei collected from rat lung tissues were pelleted by centrifugation (900 g for 15 min). Supernatants were discarded and ice-cold 0.5 N HClO₄ was added to the nuclear pellets. Acid-soluble materials were extracted and insoluble acidic pellets were discarded after centrifugation (15 min 9000 g). Supernatants were moved to fresh tubes and equal volume of 1 N KOH was added to neutralize the acid. NAD⁺ content was estimated in neutralized supernatant which was clarified by centrifugation at 9000 g for 15 min. NAD⁺ was determined via the chemical quantitation that relies on its ability to interact with acetophenone and form a compound that has a characteristic UV signal with maximum absorbance at 378 nm (Putt & Hergenrother, 2004). NAD⁺ content was defined as NAD⁺ mM/mg DNA.

Isolation and melting of DNA from lung tissues nuclear fraction. DNA was isolated from purified lung tissue nuclei according to standard protocol (Sambrook & Russel, 2001) and concentrations were measured by spectrophotometric method, using extinction coefficient $\epsilon_{260} = 6600 \text{ M}^{-1} \text{ cm}^{-1}$. Melting of DNA isolated from naked lung nuclei was performed on UV/VIS PYE Unicam-SP8-100 (UK), at the maximum wavelength 260 nm. The heating of thermostat-controlled cell (3 mL) was carried out, employing SP 876 Series 2 program device. The length of optic pathway was 1 cm. The heating rate of the thermostat-controlled cell was 0.5 °C/min and the temperature was automatically recorded in every 60 s. Data were displayed on PC monitor employing Lab View software (National Instruments, USA, 2023). Temperature and absorption data were modified and saved with Microsoft Excel Office 10 software package.

PARP 1 assay. Nuclei were gently suspended in PARP assay buffer containing 20 mM Tris, 6 mM MgCl₂, 1 mM CaCl₂, pH 7.4. Density of nuclear suspension was normalized to 1 mg DNA/mL. PARP reaction was initiated by addition of NAD⁺ stock solution to 1000 µL aliquot of nuclear suspension (0.5 mM NAD⁺ in incubation media). The reaction was carried out for 10 min at 37 °C and was stopped by centrifugation at 13000 g, 4 °C for 2 min to discard the nuclear pellets. 50 µL aliquot samples of supernatant were transferred to the Falcon UV-Vis transparent 96-well plate. Residual NAD⁺ quantitation in nuclei incubation media was performed by sequential addition of 2 M KOH, acetophenone (20% in EtOH) and 88 % formic acid, in accordance with the original assay (Putt & Hergenrother, 2004). Absorbance of PARP assay mix containing 0.5 mM NAD⁺ was measured at 378 nm. The amount of NAD⁺ was determined by using the NAD⁺ calibration curve and PARP 1 activity was defined as NAD⁺ consumed by nuclei in 10 min per mg of DNA.

In a different set of experiments PARP 1 activity was assessed after *in vitro* incubation of naked nuclei in isolation media containing BLM (10 µM) and NAD⁺ 0.5 mM within 2 hours. After incubation the nuclei were pelleted (900 g, 10 min) and supernatant was discarded. Nuclei were suspended in incubation media and precipitated (900 g, 10 min) to eliminate the input of NAD⁺ absorbed on the nuclear surfaces. This step was essential for precise control of NAD⁺ content in PARP 1 assay buffer. Final nuclear pellets were suspended in PARP 1 assay buffer and PARP 1 activity was assessed by the method described above.

PARG protein in lung nuclei. Lung nuclei were suspended in PBS and normalized to 1 mg DNA/mL. PARG protein was assessed according to recommendations of manufacturer of PARG, ELISA kit (MY Bio

Source, Inc, USA, Rat PARG ELISA kit, catalog number: MBS9336031, 2023) in 100 μ L samples of nuclear suspension. The data were presented as nanograms PARG protein per 1 mg protein. Protein was assessed with Folin-Ciocalteu reagent (Lowry et al., 1951).

Statistical analysis. For each assay, data were statistically analyzed using Statgraphics 19 SPC software package (Statgraphics Technologies, Inc., Virginia, USA, 2023). Multiple groups were compared using one-way analysis of variance (ANOVA). Results were presented as means \pm SD from 3 independent experiments. Difference in NAD⁺, PARG levels and PARP 1 activity were further analyzed using Least Significance Difference. Values $P < 0.05$ were regarded as statistically significant.

Results

PARP 1 activity. After administration of BLM to rats PARP 1 activity in nuclear fraction isolated from lung tissues decreased and dropped nearly two fold on day 8. On day 15 after BLM injection into rats PARP 1 activity was partly restored and reached nearly 70% basal PARP 1 activity.

Daily injections of TA during 7 days induced almost complete inhibition of PARP 1 activity in lung nuclei of BLM challenged rats. Within 7 days after interruption of treatment with TA PARP 1 activity was not restored to basal level (Fig. 1a).

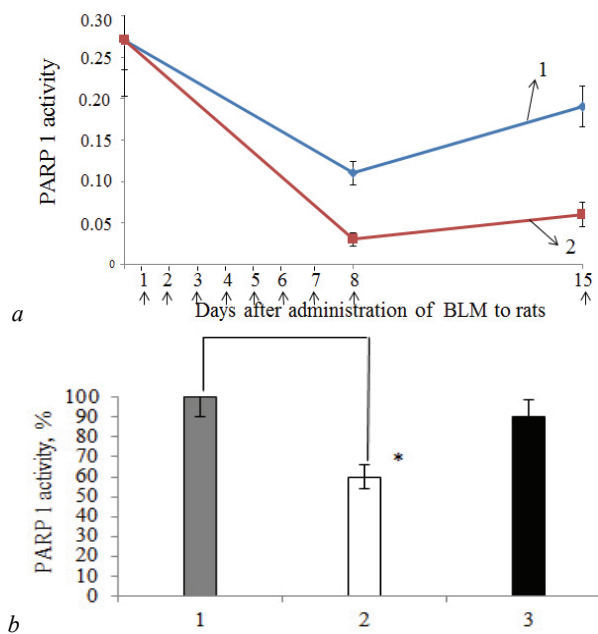


Fig. 1. PARP 1 activity in lung tissues nuclei of rats ($x \pm$ SD, $n = 4$ animals per each point on graph, duration of experiment – 23 days): *a* – rats were treated with 2 U/kg of bleomycin; 2 – daily injected with TA (10 mg/kg), arrows indicated TA injections into animals; *b* – nuclei isolated from lung tissues of control group rats and incubated *in vitro* in different incubation media; abscissa shows incubation media: 1 – nuclei isolation media, 2 – nuclei isolation media containing 10 μ M BLM; 3 – nuclei isolation media containing 10 μ M TA

The results were obtained from 3 independent experiments. A one-way analysis of variance (ANOVA) test was applied for PARP 1 activity considering $P < 0.05$ as statistically significant. In *in vitro* experimental settings lung nuclei isolated from the control group rats were exposed to BLM or to TA for 2 hours. Here, BLM induced inhibition of PARP 1 activity was observed (40% decrease), whereas TA did not affect PARP 1 activity (Fig. 1b).

DNA melting profiles. Treatment of rats with BLM did not alter melting profiles of DNA isolated from lung nuclei in 8 days after injection (Fig. 2a). When nuclei isolated from lung tissues of healthy rats were exposed to BLM added into nuclei incubation media in *in vitro* experimental settings (10 μ M), the DNA melting temperature shifted to low temperatures from 65.2 $^{\circ}$ C to 39.9 $^{\circ}$ C. The changes of ΔT decreased from 24.5 $^{\circ}$ C in control to 11.9 $^{\circ}$ C after nuclei incubation with BLM (Fig. 2b).

Intranuclear NAD⁺ and PARG protein content. Our data show that in 8 days after BLM administration to rats NAD⁺ content in the nuclear fraction collected from lung tissues dropped nearly by 25%. On day 15 after BLM injection to rats decrease in NAD⁺ content proceeded. In the case when TA was delivered to rats by systemic daily intraperitoneal injections (within 8 days after BLM administration) NAD⁺ content decreased nearly two-fold. After interruption of TA daily injections, when BLM-induced pathology was allowed to evolve for next 7 days (15 day after BLM administration) intra-nuclear NAD⁺ content tended to restore up to the level documented for the effect of BLM single injection (Fig. 3).

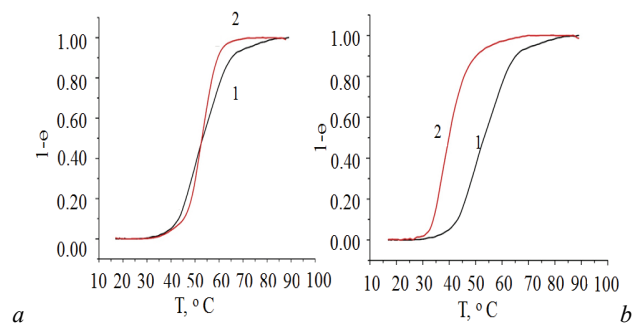


Fig. 2. Melting curves of DNA isolated from lung tissue nuclei: *a* – 1 nuclei were isolated from lungs collected from intact rats, T_m 65.5 $^{\circ}$ C; $\Delta T = 23.5$ $^{\circ}$ C; 2 – nuclei isolated from lungs of rats 8 days after BLM administration, T_m 65.3 $^{\circ}$ C; $\Delta T = 23.5$ $^{\circ}$ C; *b* – 1 nuclei isolated from lungs harvested from control group rats and incubated in isolation media for 2 hours, T_m 65.2 $^{\circ}$ C; $\Delta T = 24.5$ $^{\circ}$ C; 2 – nuclei isolated from control group rats and incubated 2 hours with 10 μ M BLM, T_m 39.9 $^{\circ}$ C; $\Delta T = 11.9$ $^{\circ}$ C; abscissa shows the melting temperature (1- θ); ANOVA test was applied for ΔT considering $P < 0.05$ as statistically significant

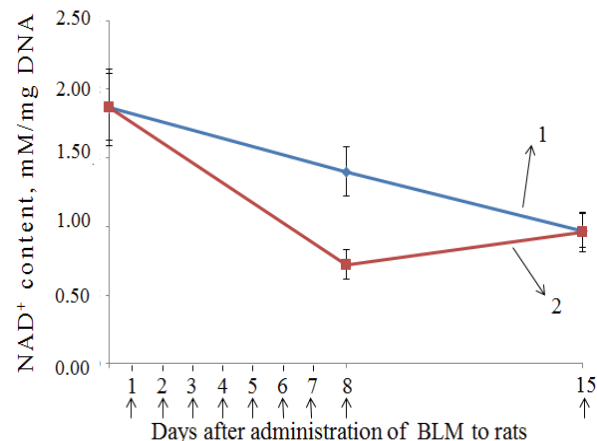


Fig. 3. NAD⁺ content in lung nuclei of rats ($x \pm$ SD, $n = 4$ animals per each point, duration of experiment – 23 days): 1 – rats treated with BLM (2 U/kg); 2 – rats co-treated with TA 10 mg/kg, arrows indicate days of TA administration; the results represent 3 independent experiments; ANOVA test was applied for NAD⁺ content considering $P < 0.05$ as statistically significant

The level of PARG protein content in lung nuclei dropped more than twofold in the 8 days after BLM administration to rats. 15 days after BLM administration to rats, PARG content returned to 75% basal level. Daily administration of TA which started 24 hours after initial treatment of rats with BLM and lasted for 7 days (8 days after BLM injection to rats) did not reliably affect dynamics of PARG protein content which were induced by BLM administration (Fig. 4).

Discussion

BLM- induced acute lung injury (ALI) rodent models are widely exploited within the scope of new anti-inflammatory and anti-fibrosis drug design. It was reported that the level of proteins PARylation increased in

lung tissues of BLM challenged mice (Lucarini et al., 2017; Szabo et al., 2020). However, considering that the level of protein PARylation is determined by complex interplay between PARP 1 and PARG, we suppose that increased PARylation in BLM-induced ALI mice lung tissues could be maintained not only by activation of polymer synthesis via PARP 1 activation, but also through down-regulation of PARp cleavage realized by PARG. Here, we were interested in examining whether BLM and anti-inflammatory natural agent TA could modulate PARP 1 enzymatic activity, PARG protein and NAD⁺ content in nuclear fraction in BLM-challenged rat lung tissues.

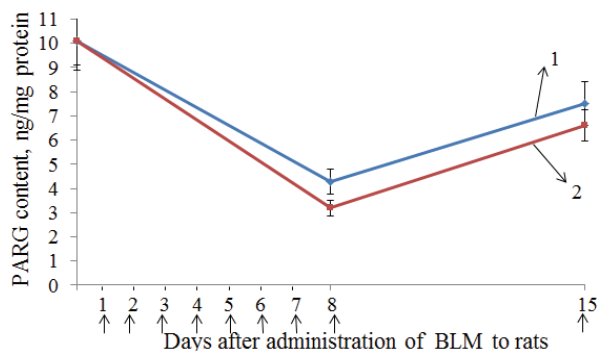


Fig. 4. PARG protein content in lung nuclei of rats treated with: 1 – BLM (2 U/kg); 2 – co-treated with TA, arrows indicate days of TA injections; $x \pm SD$, $n = 4$ animals per each point on graphic, duration of experiment – 23 days; the results represent 3 independent experiments; ANOVA test was applied for PARG content considering $P < 0.05$ as statistically significant

Our results show that in 8 days after BLM injection to rats PARP 1 activity in lung nuclei was markedly inhibited and on day 15 after BLM challenge only 70% basal enzyme activity was restored. According to these data, the development of BLM-induced inflammatory processes in lung tissues of rats were not paralleled with PARP 1 activation.

It is documented that natural hydrolysable polyphenol TA displays a broad spectrum of anti-inflammatory, neuro-protective, antitumour, cardio-protective, and anti-pathogenic effects (Wang et al., 2009; Jing et al., 2022). To study whether TA could impact PARP 1 activation pathways in rat lung tissues within the inflammatory phase of BLM-induced ALI, TA was administered to rats 24 hours after BLM challenge. Daily TA injections were continued within the next seven days and were interrupted on day 8 starting from BLM challenge. We revealed that daily injections of TA caused dramatic inhibition of PARP 1 activity in BLM-induced ALI rat lung nuclei. An assumption was made that co-treatment with BLM and anti-inflammatory agent TA in the BLM-induced ALI rat model could result in synergistic interaction between BLM and TA regarding PARP 1 inhibition. To segregate direct effects of BLM and TA on PARP 1 inhibition from the influence of other biochemical events introduced by lung inflammation we examined PARP 1 activity in naked lung nuclei collected from healthy rats and incubated *in vitro* with BLM or TA within 2 hours. Saturating physiological NAD⁺ concentration was maintained in nuclei incubation media to eliminate PARP 1 inhibition due to substrate deprivation. The results demonstrated that BLM inhibited PARP 1 activity in naked lung nuclei in *in vitro* settings. These data are in good agreement with observations documented by other investigators who observed PARP 1 inhibition by several antibiotics (Berger et al., 2017). In general, our data demonstrate that BLM-induced down-regulation of PARP 1 activity in lung nuclei was not mediated by cytosolic factors and antibiotic could directly affect PARP 1 activating pathway in nuclei. In contrast to BLM, TA did not affect PARP 1 activity in isolated lung nuclei *in vitro*. We suppose that this could result from withdrawal of certain cytosolic agents responsible for TA transport into nuclei.

It is well established that in addition to DNA single- and double-strand breaks which cease replication and transcription, BLM can bind to DNA by intercalation of its bithiazole unit between DNA bases within the DNA minor groove (Goodwin et al., 2008; Murray et al., 2018). Later it was reported that minor groove binding ligands suppress PARP1 activity (Kirsanov et al., 2014). In chromatin the drug targets DNA in linker regions of

nucleosomes (Bolzan & Bianchi, 2018), which are also recognized as preferential binding sites with PARP 1 molecules (Kim et al., 2004). Coming from this knowledge, we sought to demonstrate that BLM could down-regulate the PARP 1 activating pathway via modulating DNA structure in lung nuclei, thus disturbing the initial step in the enzyme activating pathway. For this purpose we studied melting profiles of DNA isolated from lung nuclei of BLM exposed rats. The results show that in 8 days after BLM administration the melting profile of DNA was not reliably altered. The structural changes in lung nuclei DNA became obvious when isolated lung nuclei were exposed to BLM for 2 hours in *in vitro* experimental settings. Melting curves demonstrated that DNA melting temperature shifted towards low values and ΔT significantly decreased. These modulations indicated on increased homogeneity of DNA structure and its destabilization. In concert with incomplete restoration of PARP 1 activity in 15 days after BLM treatment, our data suggest that BLM could exert a short-term effect on DNA structure in lung nuclei, which vanished in 8 days after treatment of rats with BLM. The results obtained in *in vitro* experimental settings come to show that translocation of BLM into nuclei was not mediated by any cytoplasmic factor, and support the hypothesis that BLM can suppress PARP 1 activation pathway in lung nuclei through preventing PARP 1 binding with DNA.

It is accepted that NAD⁺ provides an important link between signaling pathways and cellular metabolism. As it was reported inflammation induced a drop in cellular NAD⁺ level (Zhong & Thompson, 2006; Yang & Sauve, 2016; China et al., 2017). Apparently, the leading role in development of inflammation and lung injury could be addressed to low NAD⁺ content, which is responsible for slowing down of bioenergetics and low metabolic status of cells. Coming from this, we were interested in studying whether PARP 1 inhibition could ameliorate NAD⁺ decrease in rat lung nuclei during inflammatory phase of BLM-induced ALI. Our data show that in the 8 days after BLM was administered to rats, the NAD⁺ level in lung nuclei dropped nearly two-fold in spite of PARP 1 inhibition. These data suggest that decrease in NAD⁺ content in lung nuclei of BLM challenged rats is not coupled with PARP 1 activation. Daily treatment of rats with TA within 7 days after exposure to BLM diminished NAD⁺ content in lung nuclei two-fold. Though NAD⁺ level in lung nuclei was restored after interruption of treatment with TA a question arises whether exploitation of TA as an anti-inflammatory agent could serve as a reasonable strategy for lung anti-inflammatory therapy.

As was mentioned above, the level of protein PARylation in cells depends on dynamic interplay between PARP 1 and the PARp hydrolyzing enzyme PARG. Nevertheless, quantification of PARp had been accepted as the method of estimation of PARP 1 activity in many studies (Szabo et al., 2020), whereas the role of PARG in maintaining PARp content in cells is often undermined. Here we study the changes in PARG protein content in lung nuclei of rats in the BLM-induced ALI model.

The results show at BLM induced decrease in PARG protein content within 15 days after administration of BLM to rats. This is in good agreement with data of authors who indicated an elevated content of PARp in tissues during inflammation. We suppose that the BLM-induced decline in PARG content could be responsible for accumulation of cytotoxic PARps which provoke damage to lung cells and tissues (Andrabi et al., 2006). Nowadays, the curative potential of TA is evaluated in the context of its effect on PARG expression and accumulation of PARp in cells (Sun et al., 2012). We focused on the potential effect of TA on PARG content in lung nuclei in the initial inflammation period of BLM-induced ALI rat model. However, our data show that TA did not reliably change the dynamics of PARG content induced by BLM. Interruption of TA treatment restored NAD⁺ content to the level displayed by the lung nuclei on day 15 after BLM injection to rats. The results of the present study show that BLM and TA exhibit synergistic interaction regarding PARP 1 activity and intra-nuclear NAD⁺ content in lung nuclei. Though TA has attracted much attention in recent years due to its curative effects, the knowledge of mechanisms involved in TA effects is poor. We consider that therapeutic activity of TA could be ascribed to its chemical structure, which provide hydroxyl groups for formation of cross-links between plethora of biopolymers and macromolecules, thus acting as an effective pharmacological reagent according to a hypothesis suggested earlier (Youness et al., 2021).

Conclusions

The results of our investigation show that BLM-induced inflammation in the lungs of rats is not paralleled with PARP 1 activation. Inhibition of PARP 1 activity in lung nuclei of BLM treated rats could be maintained by the drop in NAD⁺ level and changes in DNA structure that hampered PARP 1 binding and enzyme activation. BLM translocation into lung tissues nuclei is not mediated by cytosolic factors. BLM-induced decrease in PARG content in lung nuclei could be responsible for PARp accumulation in lung cells, which serves as a death signal with destructive consequences for lung tissues. The natural anti-inflammatory agent TA elicits potentially harmful effects during BLM-induced lung inflammation displaying a synergistic effect with BLM in the field covering PARP1 activity, PARG protein and NAD⁺ content in lung nuclei.

The work was supported by the Science Committee of Republic of Armenia, in the frames of the research project No. 21T-1F014. This work was made possible by a research grant 23AN:NS-biochem-2819 from the Armenian National Science and Education Fund (ANSEF) based in New York, USA.

All authors declare that they have no known competing financial interests or personal relationships that could have appeared to influence the work reported in this paper.

References

- Andrabi, S. A., Kim, N. S., Yu, S. W., Wang, H., Koh, D. W., Sasaki, M., Klaus, J. A., Otsuka, T., Zhang, Z., Koehler, R. C., Hum, P. D., Poirier, G. G., Dawson, V. L., & Dawson, T. M. (2006). Poly(ADP-ribose) (PAR) polymer is a death signal. *Proceedings of the National Academy of Sciences of the United States of America*, 103(48), 18309–18313.
- Berger, N. A., Besson, V. C., Boulares, A. H., Bürkle, A., Chiarugi, A., Clark, R. S., Curtin, N. J., Cuzzocrea, S., Dawson, T. M., Haskó, G., Liaudet, L., Moroni, F., Pacher, P., Radermacher, P., Salzman, A. L., Snyder, S. H., Soriano, F. G., Strosznajder, R. P., Stümegi, B., Swanson, R. A., & Szabo, C. (2017). Opportunities for the repurposing of PARP inhibitors for the therapy of non-oncological diseases. *British Journal of Pharmacology*, 175(2), 192–222.
- Bolzán, A. D., & Bianchi, M. S. (2018). DNA and chromosome damage induced by bleomycin in mammalian cells: An update. *Mutation research. Reviews in Mutation Research*, 775, 51–62.
- Chinia, C. S., Tarragó, M. G., & Chinia, E. N. (2017). NAD and the aging process: Role in life, death and everything in between. *Molecular and Cellular Endocrinology*, 455, 62–74.
- Chu, X., Wang, H., Jiang, Y.-M., Zhang, Y.-Y., Bao, Y.-F., Zhang, X., Zhang, J.-P., Guo, J. H., Yang, F., Luan, Y. C., & Dong, Y.-S. (2016). Ameliorative effects of tannic acid on carbon tetrachloride-induced liver fibrosis *in vivo* and *in vitro*. *Journal of Pharmacological Sciences*, 130(1), 15–23.
- D'Amours, D., Desnoyers, S., D'Silva, I., & Poirier, G. G. (1999). Poly(ADP-ribose)ylation reactions in the regulation of nuclear functions. *Biochemical Journal*, 342, 249–268.
- Demény, M. A., & Virág, L. (2021). The PARP enzyme family and the hallmarks of cancer. Part 1. *Cell Intrinsic Hallmarks. Cancers*, 13, 2042.
- Edwards, A. D., Marecki, J. C., Byrd, A. K., Gao, J., Kevin, D., & Raney, K. D. (2021). G-quadruplex loops regulate PARP-1 enzymatic activation. *Nucleic Acids Research*, 49(1), 416–431.
- Goodwin, K. D., Lewis, M. A., Long, E. C., & Georgiadis, M. M. (2008). Crystal structure of DNA-bound Co(III) bleomycin B₂: Insights on intercalation and minor groove binding. *Proceedings of the National Academy of Sciences the United States of America*, 105(13), 5052–5056.
- Gupte, R., Liu, Z., & Kraus, W. L. (2017). PARPs and ADP-ribosylation: Recent advances linking molecular functions to biological outcomes. *Genes and Development*, 31(2), 101–126.
- Harrison, D., Gravells, P., Thompson, R., & Bryant, H. E. (2020). Poly(ADP-ribose)glycohydrolase (PARG) vs. poly(ADP-ribose)polymerase (PARP) – function in genome maintenance and relevance of inhibitors for anti-cancer therapy. *Frontiers in Molecular Biosciences*, 7, 191.
- Hewish, D. R., & Burgoyne, L. A. (1973). Chromatin sub-structure. The digestion of chromatin DNA at regularly spaced sites by a nuclear deoxyribonuclease. *Biochemical and Biophysical Research Communications*, 52(2), 504–510.
- Hopkins, T. A., Ainsworth, W. B., Ellis, P. A., Donawho, C. K., DiGiannarino, E. L., Panchal, S. C., Abraham, V. C., Algire, M. A., Yan, S., Olson, A. M., Johnson, E. F., Wilsbacher, J. L., & Maag, D. (2019). PARP1 trapping by PARP inhibitors drives cytotoxicity in both cancer cells and healthy bone marrow. *Molecular Cancer Research*, 17(2), 408–419.
- Kim, M. Y., Mauro, S., Gevry, N., Lis, J. T., & Kraus, W. L. (2004). NAD-dependent modulation of chromatin structure and transcription by nucleosome binding properties of PARP-1. *Cell*, 19(6), 803–814.
- Kirsanov, K., Kotova, E., Makhov, P., Golovine, K., Lesovaya, E. A., Kolenko, V. M., Yakubovskaya, M. G., & Tulin, A. (2014). Minor groove binding ligands disrupt PARP-1 activation pathways. *Oncotarget*, 5(2), 428–437.
- Langelier, M. F., Zandarashvili, L., Aguiar, P. M., Black, B. E., & Pascal, J. M. (2018). NAD⁺ analog reveals PARP-1 substrate-blocking mechanism and allosteric communication from catalytic center to DNA-binding domains. *Nature Communications*, 9, 844.
- Lonskaya, I., Potaman, V. N., Shlyakhtenko, L. S., Sussatcheva, E. A., Lyubchenko, Y. L., & Soldatenkov, V. A. (2005). Regulation of poly(ADP-ribose) polymerase-1 by DNA structure-specific binding. *The Journal of Biological Chemistry*, 280(17), 17076–17083.
- Lowry, O. H., Rosebrough, N. J., Farr, A. L., & Randall, R. J. (1951). Protein measurement with folin-phenol reagents. *Journal of Biological Chemistry*, 193(1), 265–275.
- Lucarini, L., Durante, M., Lanzi, C., Pini, A., Boccalini, G., Calosi, L., Moroni, F., Masini, E., & Mannaioni, G. (2017). Hydamtqi, a selective PARP-1 inhibitor, improves bleomycin-induced lung fibrosis by dampening the TGF- β /SMAD signaling pathway. *Journal of Cellular Molecular Medicine*, 21(2), 324–335.
- Murray, V., Chen, J. K., & Chung, L. H. (2018). The interaction of the metallo-glycopeptide anti-tumour drug bleomycin with DNA. *International Journal of Molecular Sciences*, 19, 1372.
- Muthurajan, U. M., Maggic, H., Hieb, A. R., Clark, N. J., Kramer, M., Yao, T., & Luger, K. (2014). Automodification switches PARP-1 function from chromatin architectural protein to histone chaperone. *Proceedings of the National Academy of Sciences of the United States of America*, 111(35), 12752–12757.
- Pazzaglia, S., & Pioli, C. (2020). Multifaceted role of PARP -1 in DNA repair and inflammation: Pathological and therapeutic implications in cancer and non-cancer diseases. *Cells*, 9(1), 41.
- Pommier, Y., O'Connor, M. J., & de Bono, J. (2016). Laying a trap to kill cancer cells: PARP inhibitors and their mechanisms of action. *Science Translational Medicine*, 8(368), 368er7.
- Putt, K. S., & Hergenrother, P. J. (2004). An enzymatic assay for poly(ADP – ribose) polymerase – 1 (PARP-1) via the chemical quantitation of NAD⁺: Application to the high-throughput screening of small molecules as potential inhibitors. *Analytical Biochemistry*, 326, 78–86.
- Reed, E. B., Ard, S., La, J., Park, C. Y., Culligan, L., Fredberg, J. J., Smolyaninova, L. V., Orlov, S. N., Chen, B., Guzy, R., Mutlu, G. M., & Dulin, N. O. (2019). Anti-fibrotic effects of tannic acid through regulation of a sustained TGF- β receptor signaling. *Respiratory Research*, 20, 168.
- Sambrook, J., & Russell, D. W. (2001). *Molecular cloning: A laboratory manual*. 3rd edition. Vol. 1. Cold Spring Harbor Laboratory Press, New York.
- Sun, Y., Zhang, T., Wang, B., Li, H., & Li, P. (2012). Tannic acid, an inhibitor of poly(ADP-Ribose) glycohydrolase, sensitizes ovarian carcinoma cells to cisplatin. *Anticancer Drugs*, 23(9), 979–990.
- Szabo, C., Martins, V., & Liaudet, L. (2020). Poly(ADP-ribose) polymerase inhibition in acute lung injury. A reemerging concept. *American Journal of Respiratory Cell and Molecular Biology*, 63(5), 571–590.
- Thomas, C., Jib, Y., Wub, C., Datz, H., Boyle, C., MacLeod, B., Patel, S., Ampofu, M., Currie, M., Harbin, J., Pechenkina, K., Lodhi, N., Johnson, S. J., & Tulin, A. V. (2019). Hit and run versus long-term activation. *Proceedings of the National Academy of Sciences of the United States of America*, 116(20), 9941–9946.
- Tulin, A., & Spradling, A. (2003). Chromatin loosening by poly(ADP)-ribose polymerase(PARP) at *Drosophila* puff loci. *Science*, 299(5606), 560–562.
- Wang, Y., Dawson, V. L., & Dawson, M. T. (2009). Poly(ADP-ribose) signals to mitochondrial AIF: A key event in parthanatos. *Experimental Neurology*, 218(2), 193–202.
- Yang, Y., & Sauve, A. A. (2016). NAD⁺ metabolism: Bioenergetics, signaling and manipulation for therapy. *Biochimica et Biophysica Acta*, 1864(12), 1787–1800.
- Jing, W., Xiaolan, C., Yu, C., Feng, Q., & Haifeng, Y. (2022). Pharmacological effects and mechanisms of tannic acid. *Biomedicine and Pharmacotherapy*, 154, 113561.
- Youness, R. A., Kamel, R., Elkasabgy, N. A., Shao, P., & Farag, M. A. (2021). Recent advances in tannic acid (gallotannin) anticancer activities and drug delivery systems for efficacy improvement. A comprehensive review. *Molecules*, 26(5), 1486.
- Zong, W. X., & Thompson, C. B. (2006). Necrotic death as a cell fate. *Genes and Development*, 20, 1–15.